Stability of modulation transfer function calibration of surface profilometers using binary pseudo-random gratings and arrays with non-ideal groove shapes

Samuel K. Barber

Lawrence Berkeley National Laboratory,

1 Cyclotron Road, M/S 2R0400,

Berkeley, CA 94720-8199, USA

+1-510-486-4077 TEL

+1-510-486-7696 FAX

Email address: SBarber@lbl.gov

Erik H. Anderson

Lawrence Berkeley National Laboratory,

1 Cyclotron Road, M/S 2R0400,

Berkeley, CA 94720-8199, USA

+1-510-486-4446 TEL

+1-510-486-4955FAX

Email address: EHAnderson@lbl.gov

Rossana Cambie

Lawrence Berkeley National Laboratory,

1 Cyclotron Road, 46R0125,

Berkeley, CA 94720-8202, USA

+1-510-486-4820 TEL

+1-510-486-4633 FAX

Email address: RCambie@lbl.gov

Stefano Marchesini

Lawrence Berkeley National Laboratory,

1 Cyclotron Road, M/S 2R0400,

Berkeley, CA 94720-8199, USA

+1-510-486-7735 TEL

+1-510-486-7696 FAX

Email address: SMarchesini@lbl.gov

Wayne R. McKinney

Lawrence Berkeley National Laboratory,

1 Cyclotron Road, M/S 2R0400,

Berkeley, CA 94720-8199, USA

+1-510-486-4395 TEL

+1-510-486-4385 FAX

Email address: WRMcKinney@lbl.gov

Peter Z. Takacs

Brookhaven National Laboratory,

Building 535B,

Utpon, NY 11973-5000, USA

+1-631-344-2824 TEL

+1-631-344-5773 FAX

Email address: Takacs@bnl.gov

Dmitry L. Voronov

Lawrence Berkeley National Laboratory,

1 Cyclotron Road, M/S 2R0400,

Berkeley, CA 94720-8199, USA

+1-510-486-4863 TEL

Email address: DLVoronov@lbl.gov

Valeriy V. Yashchuk

Lawrence Berkeley National Laboratory,

1 Cyclotron Road, M/S 2R0400,

Berkeley, CA 94720-8199, USA

+1-510-486-2592 TEL

+1-510-486-7696 FAX

Email address: VVYashchuk@lbl.gov

*Corresponding author: SBarber@lbl.gov

ABSTRACT

The major problem of measurement of a power spectral density (PSD) distribution of surface heights with surface profilometers arises due to the unknown Modulation Transfer Function (MTF) of the instruments, which tends to distort the PSD at higher spatial frequencies. The special mathematical properties of binary pseudo-random patterns make them an ideal basis for developing MTF calibration test surfaces. Two-dimensional binary pseudo-random arrays (BPRAs) have been fabricated and used for the MTF calibration of the MicroMap^{TM}-570 interferometric microscope with all available objectives. An investigation into the effects of fabrication imperfections on the quality of the MTF calibration and a procedure for accounting for such imperfections are presented.

Keywords: surface metrology, surface profilometer, interferometric microscope, modulation transfer function, power spectral density, calibration, fabrication tolerances, metrology of x-ray optics

1. INTRODUCTION

Roughness and figure specifications for state-of-the-art x-ray optics consistently push the limits of surface profilometry. In order to keep pace with growing demands of sub-Angstrom surface roughnesses and sub-micro radian slope variations, new surface profilometers and measurement techniques must be developed in parallel that achieve the desired precision.[1,2] Addressing systematic errors unique to each instrumental system is a critical step in realizing this goal. A common systematic error of a surface profilometer is the unknown impulse response, or point spread function (PSF), inherent to an instrumental setup which tends to distort measurements. The PSF is interpreted as an irradiance distribution as a function of position that convolves with an ideal image to yield a measured image. Contributions to the PSF come from various sources including, but not limited to, the instrument's optical system, detector, signal processing and software algorithm. In principle it is possible to measure or calculate the PSF of each component separately and combine them to determine the entire system's PSF.[3]

However, when correcting these distortions it is often more convenient to work in the spatial frequency domain rather than the spatial domain for several reasons. Firstly, a convolution in the spatial domain is equivalent to a multiplication in the spatial frequency domain, which is far simpler to work with. In this domain the PSF is referred to as the optical transfer function (OTF) which is generally a complex function comprised of a magnitude and phase portion called the modulation transfer function (MTF) and phase transfer function (PTF), respectively.[3] Additionally, the power spectral density (PSD) distribution of a surface under test (SUT), obtained by the square of a straightforward Fourier transform of the measured height distribution, provides a basis for a more rigorous statistical description of the surface topography than a single value obtained from roughness calculations.[4-7] For example, the measured PSD

distributions provide a closed set of data necessary for three-dimensional calculations of scattering of light by optical surfaces.[8-10] When squared, the phase portion of the OTF drops out which provides the following relation:

$$PSD_{measured} = PSD_{SUT} \times MTF^2 \tag{1}$$

The MTF in Eq. (1) is the total MTF of the instrumental system, and is a product of the individual components. As such, it provides a simple method to experimentally determine the MTF of an entire instrumental system. The MTF can be determined by comparing the measured PSD distribution of a known test surface to the ideal numerically simulated PSD distribution of the same SUT. The square root of the ratio of the measured PSD distribution to the simulated PSD distribution gives the MTF of the system.

The effectiveness of this method hinges critically on the appropriate choice of test surface. Some common test patterns used in MTF measurements include bar targets,[11] knife-edge sources,[12,13] (step height standards[14]) and white noise patterns.[15] In Refs. [16,17] a new type of test surface based on binary pseudo random (BPR) patterns has been suggested for use as a calibration standard. The effectiveness of the method was demonstrated experimentally with a BPR grating which is a one-dimensional (1D) realization of the method.[16,17] Recently, the method was expanded upon by using two-dimensional (2D) binary pseudo-random arrays (BPRAs), which are suitable for the direct measurement of the 2D MTF.[18,19] BPR surfaces have numerous advantages over other surfaces. The major distinguishing property of an ideal BPR test surface is a deterministic white-noise-like PSD distribution of the surface. This provides equal sensitivity of the MTF calibration to the entire spatial frequency range of an instrument.[16-19] However, possible fabrication imperfections of the BPRGs and BPRAs can, in principle, distort the expected ideal white-noise-like PSD distributions of the fabricated surfaces.

In the present work, we provide a comprehensive analysis on the influence of fabrication imperfections of the BPR test surfaces that may affect MTF measurement. We show that the BPRA profile imperfections characteristic of regular micro- and nano- lithography fabrication processes lead to only a 10-15% perturbation of the inherent PSD of the BPRA. This perturbation is rather insignificant if compared with the overall MTF correction that is, e.g., in the case of the MicroMap^{TM}-570 interferometric microscope, more than 2 orders of magnitude. Moreover, we show that this small perturbation of the inherent PSD of the BPRA can be analytically accounted for. The analytical methods for correction of the inherent BPRA PSD are developed and used to measure the MTF of the MicroMap^{TM}-570 interferometric microscope.

2. BINARY PSEUDO-RANDOM SEQUENCES AND ARRAYS AS TEST SURFACES

2.1 Background

Binary arrays play an important role in astronomy, where they are employed as imaging detectors for x- and gamma-ray sources. After their original conception in the late 60s,[20,21] different aperture designs were proposed and evaluated for their imaging capabilities. An important advance was made in 1978[22] with the introduction of the uniformly redundant array (URA), a design possessing both high throughput (50%) and flat PSD spectrum (when sampled at the Nyquist frequency). Tracking the mentioned similarity of the binary pseudo-random sequences and uniformly redundant arrays, we employ terms BPRG and BPRA rather than URA for the latter one, when discussing the test surfaces used for the MTF calibration.

Today the URA remains the aperture of choice for many applications, including medical imaging, plasma research, homeland security, and x-ray holography. The URA's superior imaging capability originates from the fact that its cyclical autocorrelation function is a delta function. URA’s are related by the fact that they can be constructed from binary pseudo-random

sequences. Although we have chosen the term 'binary pseudo-random sequence,' such sequences are alternatively referred to as pseudo-noise sequences or m-sequences.[23] A BPR sequence is a special type of binary sequence with a two-valued periodic autocorrelation function. It has been extensively studied in the literature.[24] What distinguishes one particular URA pattern from any other is the specific BPR sequence chosen and the details of the packing used to transform the linear array of binary numbers into a 2-D pattern. One-dimensional URAs also can be used. The URA used in this paper follows the original prescription of the twin-prime class. In its original form, the URA was configured as a rectangular aperture of dimensions $r \times s$, where r and s are prime numbers and $r = s + 2$. Thus, the matrix $A(i, j) = A(I, J)$, where $I = \mathrm{mod}_r\, i$ and $J = \mathrm{mod}_s\, j$. Furthermore,[22]

$$\begin{aligned} A(I,J) &= 0 \quad \textit{if} \quad I = 0; \\ &= 1 \quad \textit{if} \quad J = 0,\ I \neq 0; \\ &= 1 \quad \textit{if} \quad C_r(I)C_s(J) = 1; \\ &= 0 \quad \textit{otherwise}. \end{aligned} \tag{2}$$

where

$$\begin{aligned} C_r(I) &= 1 \qquad \text{if there exists an integer } x,\ 1 < x < r \\ &\qquad\qquad \text{such that } I = \mathrm{mod}_r\, x^2; \\ &= -1 \qquad \text{otherwise.} \end{aligned} \tag{3}$$

For more details see Ref. [22].

2.2 Use as MTF calibration standard

Using test surfaces based on BPR sequences and arrays has a number of advantages compared to test surfaces based on other commonly used patterns used for MTF measurements.[11-15] A bar pattern[11] can only be used for measuring the MTF at a single

fundamental spatial frequency at a time. Moreover, for each fundamental frequency, a series of measurements at harmonic frequencies needs to be made to determine the MTF at the fundamental frequency. Consequently, obtaining the MTF over a range of spatial frequencies can be a very long and tedious process requiring numerous measurements.[3,11]

In surface profilometry a knife edge source[12,13] can be modeled as a step height artifact.[14] The use of such a surface for MTF measurement of surface profilers has been presented in Ref. [14]. There are a number of disadvantages in using these surfaces. The inverse quadratic dependence of the PSD spectrum on spatial frequency limits the sensitivity to higher spatial frequency distortion. It also proves necessary to pre-process the data to filter out PSD variations at higher spatial frequencies. Furthermore, the MTF calibration exhibits a strong dependence on the position of the step height within the field of view of the instrument.

The advantage of white noise sources[15] is that the inherent PSD should be essentially flat which provides equal sensitivity to the instrumental MTF over the entire spatial frequency range. Any deviation in the measured PSD distribution from a flat PSD distribution is a direct measure of the instrumental MTF. From a practical standpoint, however, developing and using test surfaces based on generic white noise sources for MTF measurement of profiling instruments can be problematic, because white noise sources are typically not uniquely specified.

The primary property of BPR sequences and arrays that makes them an attractive option for MTF measurement test surfaces is their inherently flat (i.e. spatial frequency independent) PSD distributions. In contrast to a white noise source, this property is guaranteed by the deterministic spacing of the binary elements such that the cyclic autocorrelation function is a delta function. Therefore, BPR test surfaces are easy to specify for standard micro- and nano-fabrication processes. For our purposes a surface based on a BPR pattern is determined as a set

of rectangular grooves (of binary height levels) with grooves and peaks corresponding to values of 1 and 0 in the BPR sequence or array. As such, the PSD from a BPR grating or array is a result of the groove distribution and is not particularly sensitive to the groove shape or roughness of the groove surfaces, top or bottom. As shown in the present work, it is easy to account for any possible effect of fabrication imperfections on the spectral properties of the BPR test surface.

The suggested method involving BPR test surfaces can be adapted for a large variety of profiling instruments including interferometers, interferometric microscopes, atomic force and scanning electron microscopes[25] and scatterometers.[19] The listed advantages make BPR based test surfaces ideal for developing international MTF calibration standards.

The utility of using 1D BPR gratings for MTF calibration of the MicroMap-570^{TM} interferometric microscope has been demonstrated in Refs. [16,17]. These surfaces, however, are limited to measuring the MTF along a single direction at a time. BPRAs possess similar properties to the BPRGs with the added advantage of allowing for the direct measurement of the 2D MTF.[18,19]

3. CHARACTERIZATION OF PROTOTYPE BPRAS

3.1 Fabrication of BPRA prototypes

A set of nine prototype BPRA samples was fabricated using high-resolution electron beam lithography and Induction Coupled Plasma (ICP) etching into a silicon substrate. The datasets representing the pseudo-random patterns are generated according to the formulae presented in Sec. 2.1. The same dataset is used for all of the prototypes and consists of 4021 × 4019 elements. A value of 1 in the data set corresponds to rectangular groove in the substrate and values of 0 represent peaks, or portions that are not etched. The nine prototypes can be thought

of as three sets of three BPRAs, with each set etched to a different depth: 49 nm, 63 nm, and 122 nm. Although, in principle, etch depth should only correspond to the overall amplitude of the PSD, in a real measurement setup the etch depth may be an important factor that allows for suppression of some effects due to fabrication imperfections. Having samples etched to different depths allows one to draw a conclusion about potential effects of the imperfections. Additional information regarding the fabrication of these BPRA samples can be found in Ref. [18].

Within a set of BPRAs etched to the same depth, each BPRA is different only in regards to fundamental element size which ranges from 200 nm, to 400 nm, to 600 nm. The fundamental element size effectively determines the highest frequency up to which the PSD of the surface is expected to be flat. This frequency is equal to $1/2\Delta$, where Δ is the fundamental element size. The lower frequency bound for which the PSD of the surface is flat is determined by the total size of the surface which is equal to the product of the fundamental element size and the number of columns/rows in the BPRA. If the BPRA is measured outside of this frequency range, the PSD of the surface is no longer guaranteed to be frequency independent. Thus, a BPRA test surface should fill the entire field of view of the instrument in question, but should not be sampled at intervals shorter than the fundamental element size of the surface.

For the present work the instrument in question is the MicroMap^{TM}-570, which can be equipped with five objectives, 2.5×, 5×, 10×, 20×, and 50×. The 640 × 480 pixel imaging CCD has an effective pixel size determined by the objective in place: 3.92 μm, 1.96 μm, 0.98 μm, 0.49 μm and 0.192 μm, respectively. Thus, in principle the fabricated samples provide suitable surfaces for full aperture MTF measurement of the instrument equipped with all objectives.

3.2 General consideration of fabrication imperfections

As was mentioned in Sec. 2.2, the special mathematical properties of a BPRA are such that the PSD inherent to the test surface will have a low sensitivity to groove shape distortion.[16] However, in order to use Eq. (1) for an effective and precise MTF measurement, the PSD inherent to the test surface should be well known a priori. Consequently, it's important to consider how fabrication imperfections, particularly groove shape, will affect the inherent PSD of a given test surface.

Measurements made with the Dimension-3000 Scanning Probe Microscope (SPM) provide critical information on the surface characteristics of the BPRA samples. These measurements provide the basis for developing the theoretical models needed for the MTF calibration work. That is, the SPM data is used to estimate the groove shape distortion by means of curve fitting to a simple smoothing function with a small number of parameters. The model with the parameters found in the curve fitting is then used to calculate the inherent PSD of a model BPRA with the same groove shape. This process is discussed in greater detail in a later section.

Each of the nine BPRAs was measured under several different magnifications with the SPM. A three dimensional height distribution obtained from a typical measurement shown in Fig. 1a, depicts a 5 μm × 5 μm section of the 400 nm BPRA etched to 63 nm drawn to scale. This figure clearly reveals non-ideal sidewall profiles. In other words, the etching did not produce the desirable 90 degree sidewall slopes at the groove boundaries. Figure 1b shows a 5 μm × 5 μm array plot of the 600 nm BPRA etched to 63 nm with darker shaded regions corresponding to grooves in the substrate. This figure reveals a degree of success for the fabrication in that the shapes of the BPRA elements in the plane of the grating are highly

rectangular. Consequently, the major perturbation to the inherent PSD of the test surface will be a result of non-ideal (rounded) sidewalls.

In order to understand the affect of rounded sidewalls on the inherent PSD of a BPRA, we start with a theoretical consideration. A smoothing function can be applied to an "ideal" BPRA model to account for rounded sidewalls that mimics a "real" fabricated BPRA surface. A number of different smoothing functions can be used and the following is one example of such a function:

$$C(m) = A\sum_{-p}^{p} B(m+p)e^{-p^2/2\sigma^2}, \tag{4}$$

where $B(m)$ is the original height of the ideal profile at point m in the sequence, p is the number of points on either side of $B(m)$ to be used in smoothing, $C(m)$ is the new height of the rounded profile at point m, A is a normalization constant, and σ^2 determines the 'strength' of the smoothing function. The free parameters σ^2 and p can be adjusted to vary the shape distortion from very slight rounding to relatively large distortions. Figure 2a shows 1D height profile traces of the first few elements from several BPRA models in which only the strength of rounding has been varied. These models were created using a fundamental element size of 0.6 units, which corresponds to a Nyquist frequency of ~0.8 units.$^{-1}$ The calculated PSDs from these models are shown in Fig. 2b. Although the data presented in Fig. 2 show only a small portion of the numerical models created and analyzed, the results are typical.

3.3 MicroMap™-570 measurements

In general, it cannot be expected that an entire BPRA fits perfectly within the field of view of the microscope. In most cases only a portion of the BPRA falls in the field of view. It

was shown in Ref. [17] that averaging the PSD spectra of multiple measurements, obtained by successively shifting the field of view to different portions of a SUT, accurately recovers the PSD spectrum of the surface. Additionally, averaging several measurements significantly reduces the noise. Of course, the range of spatial frequencies in the measured PSD spectrum is defined by the total size of the field of view in the lower end and by the effective pixel size in the higher end. It is important to make the distinction between the detectable spatial frequency range and the spatial frequency range used to describe the BPRA. For the BPRA, the spatial frequency range is determined as the range over which the PSD is invariant. The detectable range will generally be just a portion of the BPRA frequency range, being cutoff in the low frequency range by the size of the detector and in the high frequency range by the detector effective pixel size.

Each of the nine BPRAs was measured with MicroMap^{TM}-570 interferometric microscope equipped with all five objectives. Using PSD software developed at the ALS OML,[5-7] the 2D PSD is calculated for each surface. The software includes the option to average the PSDs from several different measurements. For ease of visualization, the 2D PSDs have been integrated along the x and y directions to produce two 1D PSDs along the y and x directions, respectively. Figures 3 and 4 show the results of these PSD calculations for 400 nm BPRA with the 122 nm etch depth and the 600 nm BPRA with the 49 nm etch depth, respectively.

The PSDs exhibit a relatively high degree of flatness at the lowest spatial frequencies for each given objective. As the frequency increases, however, there is a rather quick and steep roll off of the PSD of several orders of magnitude. This data clearly demonstrates the major impact of the instrumental MTF and the need to calibrate this effect. Only at a small number of the lowest spatial frequencies for a given objective do the PSDs appear to be unaffected by the instrumental MTF.

The PSDs in Fig. 4 obtained from a shallower etched BPRA do not exhibit the same degree of flatness in the low spatial frequency ranges as those in Fig. 3. As was noted in Sec. 3.1, a difference in etch depth should really only manifest itself in the PSD as an overall shift of the PSD amplitude. These raised low frequency tails start to flatten out as the magnification is increased. Upon examining the height distribution data obtained directly from MicroMap^{TM}-570 measurements, the source of these perturbations becomes clear.

Figure 5 shows height distribution measurements of the silicon substrate next to one of the samples and of the 600 nm BPRA with 43 nm etch depth. The measurements were made with MicroMap^{TM}-570 when equipped with the 5× objective. The measurement of the silicon substrate, Fig. 5a, clearly reveals low frequency surface variations in the silicon substrate with peak to valley values on the order of 8 nm. When examining the height distribution of the BPRA, Fig. 5b, along with the BPR pattern, the surface variations of the silicon substrate also show through. Evidently, when the etch depth is not sufficiently deep, the inherent waviness of the silicon wafer distorts the measured PSDs, particularly in the low frequency range. This effect is not noticed when measuring with higher magnification objectives as these low frequency contributions are cut off.

Because similar raised low frequency tails are not noticeable in Fig. 3, it is possible to conclude that etch depths of 122 nm are deep enough to suppress perturbations due the silicon substrate's surface variations. For future samples, a better approach than setting limits on etch depth would be to start with higher quality polished substrates.

4. AB INITIO MTF CALIBRATION

4.1 BPRA modeling

The process of calibrating the MTF of the MicroMap^{TM}-570 necessarily begins by estimating the perturbation to the inherent PSDs of the BPRAs due to groove shape distortion resulting from the fabrication process. As mentioned in Sec. 3.3, this is completed by means of curve fitting SPM data. Of the three sets of BPRAs, the samples etched to 63 nm yielded the highest quality SPM data. That is, the height traces exhibit the smoothest and most consistent height distributions, which allow the most accurate modeling. For this reason, the 200 nm, 400 nm, and 600 nm BPRAs etched to 63 nm were chosen for an ab initio approach to the MTF correction.

The fitting procedure used to estimate the groove shape begins by taking a trace of the height profile of a single peak to groove boundary from the SPM data, see Fig. 6a. The first step is to create a new dataset that is an "ideal" representation of the real BPRA sample. This can be accomplished by forcing the SPM height profile to binary height levels using a threshold height. Above the threshold height the "ideal" dataset will have a value equal to the average peak height, below the threshold the value will be 0, see Fig. 6b. A smoothing function is then applied to the "ideal" dataset that approximates the rounding. The function used here is the same as Eq. (4). The free parameters σ^2 and p are varied and the best fit parameters are determined by minimization of the mean root square deviation, see Fig. 6c. Using different height profiles from different portions of the SPM data, the same fitting procedure is repeated. The final best fit parameters are found as the average of the best fit parameters found in the individual fitting

routines. In this way best fit parameters were calculated from the SPM data obtained from the 600 nm BPRA etched to 63 nm.

A model BPRA was created based using the above prescriptions and the corresponding 2D PSD inherent to the particular realization of the BPRA sample was calculated. It was found that the inherent PSD is expected to deviate from a flat PSD by ~15% at the highest frequency, determined by the fundamental element size, of the BPRA. In the detectable range of the measurement system, as determined by the objective, the deviation from a flat PSD can be considerably less. For example, the highest spatial frequency of a 600 nm BPRA is 0.833 $\mu m.^{-1}$ The highest detectable spatial frequency of the MicroMap^{TM}-570 when equipped with the 10× objective (effective pixel size 0.98 μm) is ~0.5 $\mu m.^{-1}$ At this spatial frequency, the deviation from a flat PSD is only about 8%.

4.2 MTF calibration of MicroMap^{TM}-570 interferometric microscope

For an ab initio calibration, we use the MTF that is directly found as the square root of the ratio of the measured 2D PSD to the 'theoretical' 2D PSD, which is calculated using the BPRA model of the 600 nm BPRA etched to 63 nm. In order to relate the PSD measured by the MicroMap^{TM}-570 to the PSD calculated from the theoretical model, additional considerations are needed. The PSDs from the BPRA models presented up to this point correspond to measuring a real BPRA in which the detector has the exact same number of pixels as the BPRA has elements and in which the detector is aligned such that each pixel perfectly maps to a single element of the BPRA. Such a system would be an ideal measuring system, which is essentially an impossible scenario in a real lab setting. The MicroMap^{TM}-570 detector has 640 × 480 pixels, with an effective pixel size that varies with the objective being used. This results in two differences from

the ideal scenario. First, the entire field of view, for the majority of the cases, will be smaller than the BPRA. Second, for BPRAs presented in this work, a single pixel in the detector may 'see' just a portion of, or more than, one element of the BPRA.

Accordingly, the theoretical PSD is calculated in a way that reflects how real measurements are made. To account for the effective pixel size of the detector, we apply a simple convolution procedure. For example, for the 10× objective, the effective pixel size of the detector is 0.98 μm × 0.98 μm. We convolve the model by calculating the average height for each adjacent section of 0.98 μm × 0.98 μm of the model. After the convolution, several sections of 640 × 480 points are extracted from the convolved model, which represents taking several measurements with the MicroMap^{TM}-570 equipped with the 10× objective. The final 2D PSD is then calculated by averaging the 2D PSDs of the individual sections.

Using the theoretical PSD calculated from the preceding example, the two dimensional MTF has been experimentally determined for the MicroMap^{TM}-570 equipped with the 10× objective. Again, this is achieved by dividing the measured PSD of the sample by the calculated theoretical PSD of the sample and taking the square root. For visualization purposes the measured 2D MTF was integrated along each direction and is shown in Fig. 7. From a qualitative standpoint the MTF results exhibit precisely the expected characteristics. Namely, there is negligible modulation of the measured signal in low frequency range, but at the highest frequencies, the signal is considerably modulated to less than %20 of the expected value. Furthermore, PSD measurements, which are a product of the signal and the MTF squared, are reduced to less than %4 of the expected value at the highest frequencies.

The MTF found in this way was then used to correct measurements made with the 10x objective of the other BPRAs (200 nm and 400 nm) with the same etch depth, Fig. 8. The lower

curves are the un-corrected curves and the top curves have been divided by the MTF squared. These results offer a good indication of success. The PSDs inherent to these BPRAs are expected to be largely flat across the entire detectable spatial frequency range. The corrected PSDs clearly demonstrate that the when the experimentally determined instrumental MTF has been accounted for, the recovered PSD exhibits precisely the expected characteristics that are guaranteed by the mathematical properties of the BPRAs. Note that a roll off of more than three orders of magnitude in the high frequency range of the PSDs has been corrected when the MTF calibration is applied. These results provide verification that the proposed method and corresponding test surfaces are suitable for direct two-dimensional MTF calibration across the entire spatial frequency bandwidth of the instrument in question.

An interesting result of applying the MTF correction to these measurements is that the value of the RMS roughness, which is directly proportional to the square root of the integrated PSD, changes drastically. For the case of the 400 nm BPRA, Fig. 8, the directly measured RMS roughness is 6 nm compared with a roughness of 15 nm obtained after the MTF calibration has been applied. One should expect a change of the roughness number after the MTF correction has been applied, particularly for surfaces with random distributions of surface height, like the BPRAs. For optics, however, which generally have a fractal like 1D PSD that decreases sharply with increasing spatial frequency,[26] the PSD distribution at high spatial frequencies does not significantly contribute to the overall roughness. As such, applying the MTF correction to such an optic will not drastically alter the roughness value.

In the straightforward application of the proposed method, as has been done for an illustrative purpose throughout the present work, the MTF found tends to be noisy. This is related to the fact that the MTF is found by dividing a measured PSD by a simulated PSD, which

each have inherent noise. Consequently, the PSDs with the MTF correction applied are significantly noisier than the original measurements, Fig. 8. The influence of noise can be simply suppressed by averaging over multiple measurements performed over different areas of the test surface.[16,17] In the present case, only four such measurements were made. Another way to get a smoother MTF distribution of a profilometer is to fit the measured MTF to an analytical model[19] with the fabrication imperfection analytically accounted for. Such a description of the MTF allows evaluation of the effective pixel size of the instrument and, therefore, its real Nyquist frequency.

5. CONCLUSION

Test surfaces based on binary pseudo-random arrays have been fabricated and their applicability for calibration of the two dimensional MTF of an interferometric microscope has been investigated. Special considerations have been made to account for effects on the calibration of a non-ideal (deviated from an ideal rectangular) profile of the array elements. The profile non-ideality appears to be due to the imperfections of the used fabrication processes. The inclusion of fabrication imperfections in BPRA models is generally characterized by a high frequency roll off in the PSD of about 10-15% with little to no effect at lower spatial frequencies. Because the range of detectable spatial frequencies is limited by the measuring system, much of the effect of fabrication imperfections seen at higher spatial frequencies of the test surface is not detectable in the course of the MTF calibration.

The profile distortion was measured with a scanning probe microscope. It has been shown that the measured surface profile can be sufficiently approximated with a simple analytical model. The approximation allows for numerical evaluation of the inherent PSD of the

fabricated test surface. The found inherent PSD is used to precisely calibrate the profilometer MTF with a total accounting of the non-ideality of the fabricated test surface.

As an example, results of measuring the MTF of the MicroMap^{TM}-570 equipped with the 10× objective using the 600 nm BPRA etched to 63 nm as a reference surface have been presented. Using the experimentally determined MTF, measurements of the other BRPA's (200 nm, 400 nm) have been corrected. The corrected PSDs exhibit precisely the characteristics that are expected for such surfaces, providing conclusive evidence of the applicability of this MTF calibration procedure for precise MTF calibration of the interferometric microscope.

In summary, the investigations performed here have demonstrated a low sensitivity of modulation transfer function calibration using binary pseudo-random gratings and arrays to the groove shape perturbation due to fabrication imperfections. This is because the inherent PSD of a BPRA is a result of the distribution of its elements rather than the element shape. Therefore, the BPRA test surfaces precisely satisfy the requirements of ease of specification and reproducibility of the test surfaces when used as a certified standard.

Note that further improvement of the fabrication technology directed to develop BPR test surfaces with rectangular, or very nearly rectangular, edges is possible.[18] In this case, the considered correction procedure can be omitted; and direct MTF calibration with an accuracy of about 1% can be obtained.

The developed analytical methods of correction of the inherent PSD distribution of a BPRA are useful when specifying the fabrication tolerances of BPR test surfaces suitable for calibration of instruments with significantly smaller (e.g., for scanning electron and atomic force microscopes) and larger (e.g., for large area interferometers) fields of view than that of the

interferometric microscope used in the present investigation. The work to develop such test surfaces is in progress.

ACKNOWLEDGEMENTS

The authors are grateful Howard Padmore for extremely useful discussions. The Advanced Light Source is supported by the Director, Office of Science, Office of Basic Energy Sciences, Material Science Division, of the U.S. Department of Energy under Contract No. DE-AC02-05CH11231 at Lawrence Berkeley National Laboratory.

DISCLAIMER

References

1. L. Assoufid, O. Hignette, M. Howells, S. C. Irick, H. Lammert, and P. Z. Takacs, "Future metrology needs for synchrotron radiation grazing-incidence optics," *Nucl. Instr. and Meth. .A* **467-468**, 267-70 (2001).

2. P. Z. Takacs, "X-Ray Mirror Metrology," in M. Bass (Ed.), *Handbook of Optics*, third ed., vol. V, chapter 46, McGraw-Hill Publishing Company, New York (2009).

3. G. D. Boreman, *Modulation Transfer Function in Optical and Electro-optical Systems*, SPIE Press, Bellingham (2001).

4. R. N. Bracewell, *The Fourier Transform and Its Applications*, McGraw-Hill Publishing Company, New York (1986).

5. V. V. Yashchuk, A. D. Franck, S. C. Irick, M. R. Howells, A. A. MacDowell, W. R. McKinney, "Two dimensional power spectral density measurements of x-ray optics with the MicroMap interferometric microscope," *Proc. SPIE* **5858**, pp. 58580A-1-12 (2005).

6. V. V. Yashchuk, S. C. Irick, E. M. Gullikson, M. R. Howells, A. A. MacDowell, W. R. McKinney, F. Salmassi, T. Warwick, "Cross-check of different techniques for two dimensional power spectral density measurements of x-ray optics," *Proc. SPIE* **5921**, pp. 59210G-1-12 (2005).

7. V. V. Yashchuk, E. M. Gullikson, M. R. Howells, S. C. Irick, A. A. MacDowell, W. R. McKinney, F. Salmassi, T. Warwick, J. P. Metz, T. W. Tonnessen, "Surface roughness of stainless-steel mirrors for focusing soft x rays," *Appl. Opt.* **45**(20), 4833-42 (2006).

8. Church, E. L., Jenkinson, H. A. and Zavada, J. M., "Relationship between surface scattering and microtopographic features," *Opt. Eng.* **18**(2), 125-36 (1979).

9. J. C. Stover, *Optical Scattering*, second edition, SPIE Optical Engineering Press, Bellingham (1995).

10. D. Attwood, *Soft X-rays and Extreme Ultraviolet Radiation*, Cambridge University Press, New York (1999).

11. G. D. Boreman and S. Yang, "Modulation transfer function measurement using three- and four-bar targets," *Appl. Opt.* **34**, pp. 8050-8052 (1995).

12. R. Barakat, "Determination of the optical transfer function directly from the edge spread function," *Journal of the Optical Society of America* **55**, 1217-1219 (1965).

13. B. Tatian, "Method for obtaining the transfer function from the edge response function," *Journal of the Optical Society of America* **55**, 1014-1019 (1965).

14. P. Z. Takacs, M. X. Li, K. Furenlid, E. L. Church, "Step-height standard for surface-profiler calibration," *Proc. SPIE* **1995**, 235-44 (1993).

15. A. Daniels, G. D. Boreman, A. Ducharme, and E. Sapir, "Random transparency targets for modulation transfer function measurement in the visible and IR," *Opt.l Eng.* **34**, 860-868 (1995).

16. V. V. Yashchuk, W. R. McKinney, and P. Z. Takacs, "Binary Pseudorandom Grating Standard for Calibration of Surface Profilometers," *Opt. Eng.* **47**(7), 073602-1-5 (2008).

17. V. V. Yashchuk, W. R. McKinney, and P. Z. Takacs, "Binary Pseudorandom Grating as a Standard Test Surface for measurement of Modulation Transfer Function of Interferometric Microscopes," *Proc. SPIE* **6704**, 670408/1-12 (2007).

18. S. K. Barber, P. Soldate, E. D. Anderson, R. Cambie, W. R. McKinney, P. Z. Takacs, D. L. Voronov, and V. V. Yashchuk, "Development of Pseudo-random Binary Gratings and Arrays

for Calibration of Surface Profile Metrology Tools," *J. Vac. Sci. and Tech. B* **27**(6), 3213-9 (2009).

19. S. K. Barber, E.D. Anderson, R. Cambie, W. R. McKinney, P. Z. Takacs, J. C. Stover, D. L. Voronov, and V. V. Yashchuk, "Binary Pseudo-Random Gratings and Arrays for Calibration of Modulation Transfer Function of Surface Profilometers," *Nucl. Instr. and Meth. .A* (2009), doi:10.1016/j.nima.2009.11.046.

20. R. H. Dicke, "Scatter-hole cameras for X-rays and gamma rays," *Astrophysics Journal* **153**, L101–L106 (1968).

21. J. G. Ables, "Fourier transform photography: a new method for X-ray astronomy," *Proc. of the Astronomical Society of Australia* **1**, 172–173 (1968).

22. E. E. Fenimore, and T. M. Cannon, "Coded aperture imaging with uniformly redundant arrays," *Appl. Opt.* **17**(3), 337-47 (1978).

23. P. H. Bardell, W. H. McAnney, and J. Savir, *Built-in test for VLSI pseudorandom techniques*, John Wiley and Sons Inc., New York (1987).

24. S. Marchesini, S. Boutet, A. E. Sakdinawat, M. J. Bogan, S. Bajt, A. Barty, H. N. Chapman, M. Frank, S. P. Hau-Riege, A. Szöke, C. Cui, D. A. Shapiro, M. R. Howells, J. C. H. Spence, J. W. Shaevitz, J. Y. Lee, J. Hajdu, and M. M. Seibert, "Massively parallel X-ray holography," *Nature Photonics* **2**, 560–563 (2008).

25. The corresponding developments and experiments are in progress at the Advanced Light Source (ALS) Optical Metrology Laboratory (OML).

26. E. L. Church, "Fractal surface finish," *Appl. Opt.* **27**(8), 1518-1526, (1988).

Biographies

Samuel K. Barber received his BS degree in Physics with a minor in Spanish from the University of California at Los Angeles in 2007. He then completed a brief fellowship at the Laboratori Nazionali di Frascati, Italy, where he assisted in the design and simulation of quadrupole and dipole magnets. He is currently working in the Optical Metrology Laboratory at the Advanced Light Source, Lawrence Berkeley National Laboratory. His current research interest is in x-ray optical instrumentation and metrology.

Erik H. Anderson attended the Massachusetts Institute of Technology in Cambridge Mass, USA and received BS in 1981, MS in 1984 and PhD in 1988 all in the Department of Electrical Engineering and computer science. He joined Lawrence Berkeley National Laboratory in 1988 and worked as a visiting scientist at the IBM T.J. Watson Research Laboratory in Yorktown Heights New York developing zone plate optics for x-ray microscopy. In 1993 he moved to Berkeley to build and manage the Nanofabrication facility, within the Center for X-Ray Optics. He is currently involved in EUV and soft x-ray optics development, characterization, e-beam lithography, Nanofabrication, and x-ray microscopy.

Rossana Cambié received a Master of Science degree and PhD in Electrical Engineering from the University of Pavia (Italy) finishing in 2003 with a thesis in Micro-Electro-Mechanical System (MEMS) technology and applications in collaboration with ST Microelectronics in Milan, Italy. Rossana has been with the Lawrence Berkeley National Laboratory since 2003 where she provides expertise in micro and nano-fabrication process development and optimization to the Center of Systems Biology Engineering. Her current research interests are in instrumentation and metrology for x-ray optics and detectors, in-focus phase contrast for electron microscopy, cryo-EM, micro and nanofluidic systems and plasmonic applications.

Stefano Marchesini received his MS degree in Physics from the University of Parma (Italy, 1995) and his PhD degree from the University J. Fourier of Grenoble (France, 2000). He then worked at Lawrence Livermore and Lawrence Berkeley National Labs where he worked on x-ray imaging technologies. His current research interests are in coherent x-ray scattering, holography, coded apertures, optics and image processing.

Wayne R. McKinney received his BA, MA, and PhD in Physics from The Johns Hopkins University, finishing in 1974 with a thesis in ultraviolet astronomy. He then completed a post-doctoral appointment in molecular biology supported by a National Cancer Institute Fellowship at the Biology Department of Brookhaven National Laboratory in 1977. Remaining at Brookhaven from 1977 to 1979 in the Instrumentation Division he designed optical systems for the National Synchrotron Light Source. From 1979 to 1987 he joined the research staff of the Richardson Grating Lab in Rochester New York, becoming Manager of Diffraction Grating R&D in 1981. From 1987 to 1989 he was a staff scientist in the Center for X-Ray Optics at Lawrence Berkeley National Laboratory working on water cooled optical components and monochromator designs for the Advanced Light Source. This work won local and national Tech Transfer Awards, and led to Fellow status in the OSA. He now works directly for the Advanced Light Source where he designed and built the first infrared beamlines. Currently his responsibilities are in optical metrology, particularly the specification of x-ray optics by calculation of scattering.

Peter Z. Takacs directs the activities of the Optical Metrology Laboratory in the Instrumentation Division of Brookhaven National Laboratory. He is actively involved in the development of instrumentation, methods, and standards used for testing the figure and finish of aspheric optics, such as those used for reflecting x-rays at grazing incidence. He received a BA

from Rutgers University in 1969 and a PhD in physics from Johns Hopkins University in 1974. He received an R&D 100 Award and a Photonics Spectra Circle of Excellence Award in 1993 for development of the Long Trace Profiler.

Dmitriy L. Voronov received his MS degree in physics of metals and semiconductors from Kharkov Polytechnic Institute in 1989, and his PhD degree from Kharkov National University (Ukraine) in 2003. He is an author of more than 20 publications in the fields of EUV multilayer mirrors, interdiffusion and phase transformation in metal-silicon thing films. He currently works for the Advanced Light Source, Lawrence Berkeley National Laboratory. His current research is focused on development of high efficiency and high resolution diffraction gratings for EUV and soft x-rays.

Valeriy V. Yashchuk received his MS degree in experimental physics from St. Petersburg State University (Russia) in 1979, and his PhD degree from St. Petersburg Nuclear Physics Institute (Russia) in 1994. He is currently leading the Optical Metrology Laboratory at the Advanced Light Source, Lawrence Berkeley National Laboratory. He has authored more than 60 scientific articles in the fields of atomic and molecular physics, nonlinear optics, electro- and magneto-optics, laser spectroscopy, experimental scientific methods and instrumentation, and optical metrology. In 1986 for the development of a method of reduction of phase space of an atomic beam he was awarded the Leningrad Komsomol Prize in physics. In 2007, he received R&D Magazine's R&D 100 Award for development of Laser-Detected MRI. His current research interest is in x-ray optics, optical instrumentation and metrology for x-ray optics.

Figure captions:

Figure 1: 3D height distribution of a 5 μm × 5 μm section of the 400 nm BPRA, etch depth 63 nm, as measured with the SPM, (a). 2D height distribution array plot of 5 μm × 5 μm section of the 600 nm BPRA, etch depth 63 nm, as measured with the SPM, (b). Dark shaded regions represent grooves in the substrate.

Figure 2: One dimensional height profiles of the first few elements of model BPRAs with different degrees of rounding, (a). The rounded edges approximate fabrication imperfections of "real" BPRAs. Calculated 1D PSDs are shown in (b). The curves with increasing deviations from flat at the higher spatial frequencies correspond to the models with increasing rounding.

Figure 3: 1D PSDs obtained by integration along the sagittal, (a) and tangential, (b), directions of the measured 2D PSD of the 400 nm BPRA etched to 122 nm. Measurements were made with the MicroMap^{TM}-570 equipped with 2.5×, 5×, 10×, 20×, and 50× objectives (lines (1), (2), (3), (4) and (5), respectively). The PSDs exhibit a high degree of flatness in the low spatial frequency range, but the steep high frequency roll off clearly demonstrates the need to calibrate the MTF effect.

Figure 4: 1D PSDs obtained by integration along the sagittal, (a) and tangential, (b), directions of the measured 2D PSD of the 600 nm BPRA etched to 43 nm. Measurements were made with the MicroMap^{TM}-570 equipped with 2.5×, 5×, 10×, 20×, and 50× objectives (lines (1), (2), (3), (4) and (5), respectively). The raised low frequency tails clearly visible PSDs from the 2.5× and 5× objectives indicate the contribution of low frequency surface variations of the inexpensive silicon wafer into which the BPRAs are etched. For the higher magnification objectives, these contributions are not noticed and the PSDs are relatively flat in the low spatial frequency ranges.

Figure 5: MicroMap^{TM}-570 measurements with the 5× objective of the bare silicon surface (a) and shallow 49 nm etch depth 600 nm BPRA (b). The large-scale roughness of a standard silicon wafer is evident at lower spatial frequencies. The low frequency roughness limits the use of these reference samples in calibrating the 2.5× and 5× objectives. Polished silicon flats should not have this roughness.

Figure 6: Viewgraphs illustrating the different steps in the curve fitting procedure used to develop a best fit model of the real BPRA sample. A height profile from the SPM data of a single peak to groove boundary, (a). A dataset representing an "ideal" BPRA, solid line, is created by forcing the SPM data to binary height levels using a threshold height, dotted line, (b). A smoothing function, like that of Eq. (4), is applied to the "ideal" dataset to approximate the rounding of the real BPRA sample, (c).

Figure 7: MTF results obtained after taking the square of the ratio of the measured 2D PSD to the theoretical PSD. The 2D MTF has been integrated along the sagittal (a) and tangential (b) direction for visualization purposes.

Figure 8: Measured (lines marked "1") and MTF corrected (lines marked "2") 1D PSDs of the 400 nm BPRA, (a) and 200 nm BPRA, (b) with 63 nm etch depth. Measurements were made with the MicroMap^{TM}-570 using the 10× objective. For (a) the PSD is along the tangential direction and for (b) the PSD is along the sagittal direction. Corrected PSDs are virtually flat across the entire frequency range.

Figures

1. 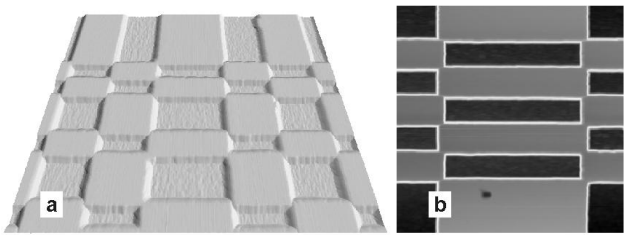
a
b

2. 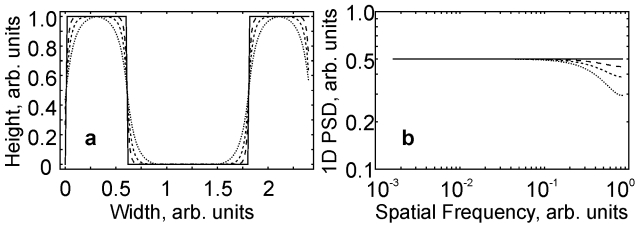
Height, arb. units
1.0
0.8
0.6
0.4
0.2
0
a
0
0.5
1
1.5
2
Width, arb. units
1D PSD, arb. units
1.0
0.5
0.2
0.1
b
10^{-3}
10^{-2}
10^{-1}
10^{0}
Spatial Frequency, arb. units

3. 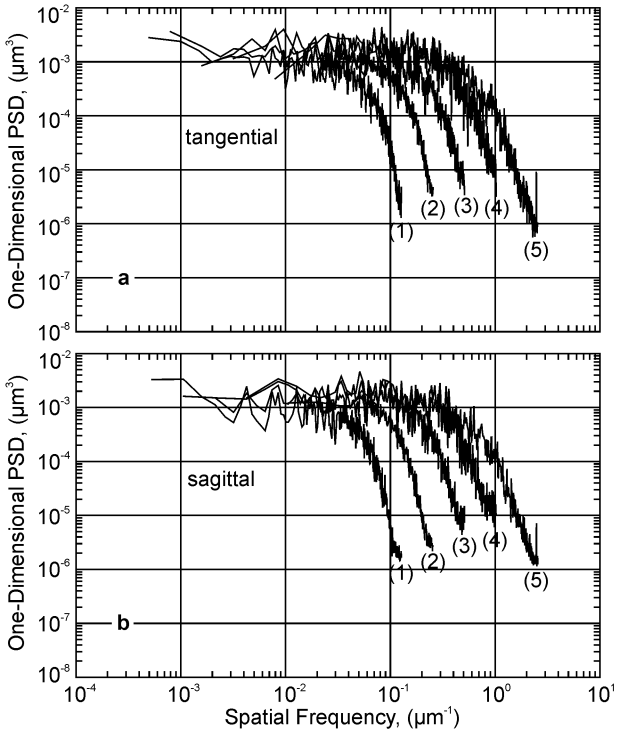
One-Dimensional PSD, (μm^3)
tangential
(1)
(2)
(3)
(4)
(5)
a
sagittal
b
10^{-4}
10^{-3}
10^{-2}
10^{-1}
10^{0}
10^{1}
Spatial Frequency, (μm^{-1})

4.

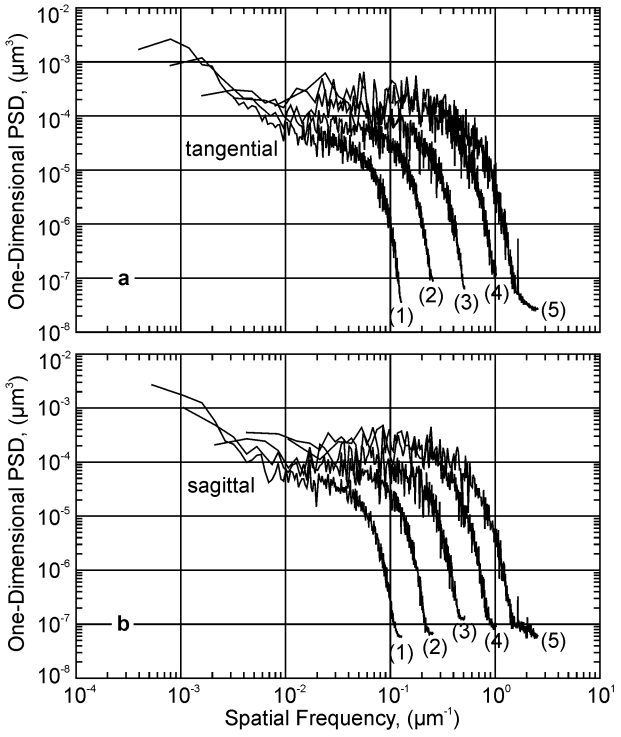
One-Dimensional PSD, (μm³)
tangential
a
(1)
(2)
(3)
(4)
(5)
sagittal
b
Spatial Frequency, (μm⁻¹)

5.

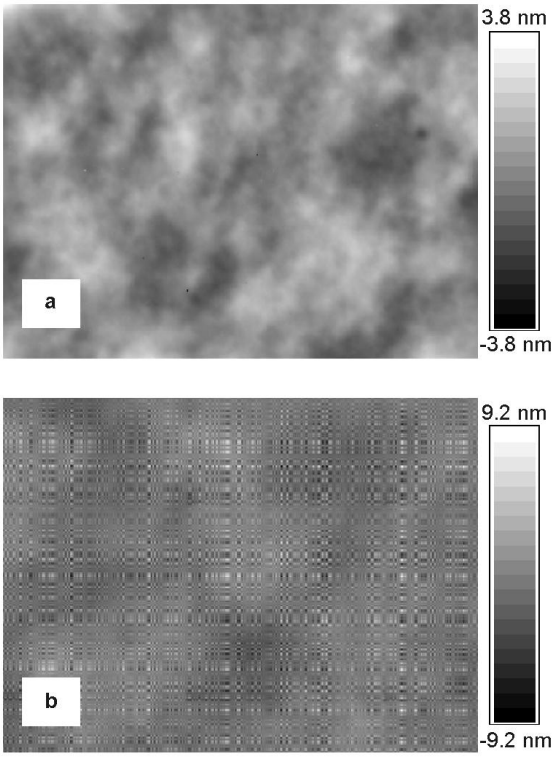
3.8 nm
-3.8 nm
a
9.2 nm
-9.2 nm
b

6.

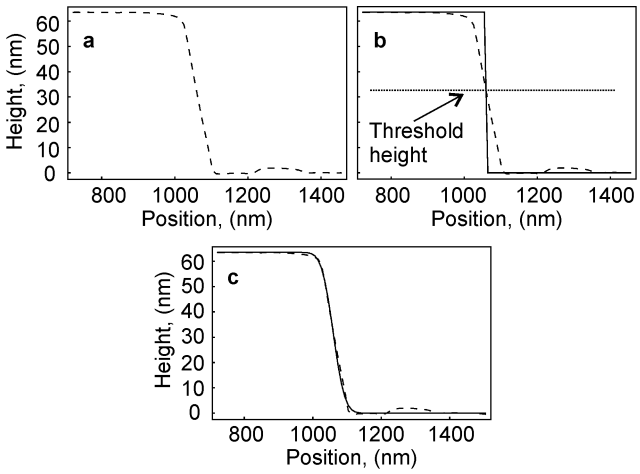
a
b
c
Height, (nm)
Position, (nm)
Threshold
height
60
50
40
30
20
10
0
800
1000
1200
1400

7.

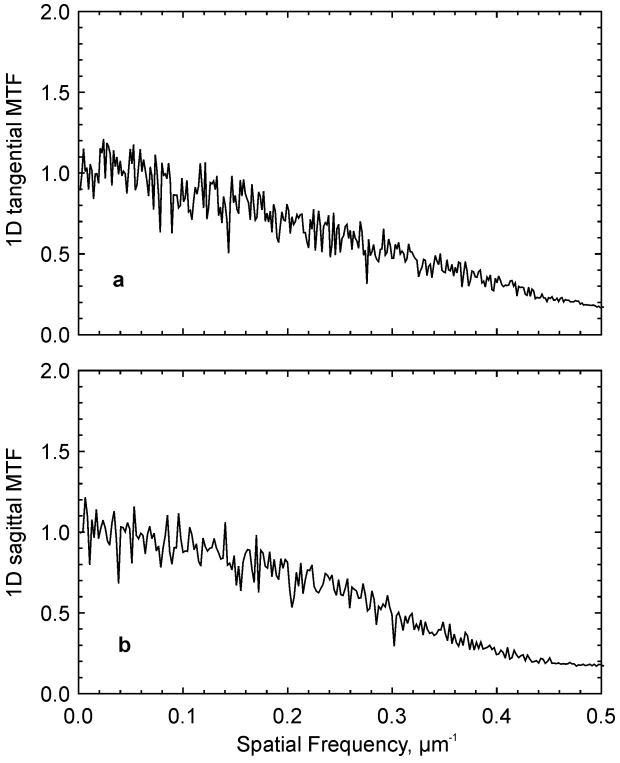
1D tangential MTF
1D sagittal MTF
a
b
2.0
1.5
1.0
0.5
0.0
0.1
0.2
0.3
0.4
0.5
Spatial Frequency, μm-1

8.

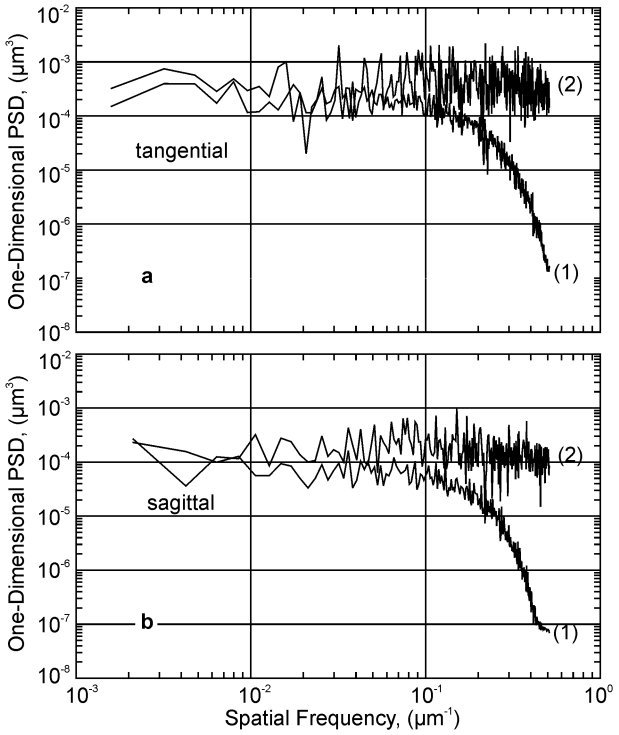
One-Dimensional PSD, (μm³)
tangential
(2)
(1)
a
sagittal
b
Spatial Frequency, (μm⁻¹)